CMS EXPERIMENT

A.A.Vorobyov, V.L.Golovtsov, Yu.M.Ivanov, D.M.Seliverstov

1. Introduction

The Compact Muon Solenoid experiment (CMS) is a general-purpose detector designed to exploit the physics of proton-proton collisions at centre-of mass energy of 14 TeV over the full range of luminosities expected at the LHC.

The primary objectives of CMS experiment are:

– Search for the Standard Model Higgs Boson.
– Search for various Supersymmetric Model Higgs Boson.
– Search for supersymmetric particles (squarks, gluinos, ...).
– In the absence of elementary Higgs particle(s), search for a strong-coupling scenario based on dynamic symmetry breaking. Detailed studies of WW, WZ, ZZ final states.
– Search for new heavy gauge bosons (Z', ...).
– Top-quark physics.

CMS is planning also studies of CP violation in the B-sector, observation of B_s^0-oscillations and possible signals for QCD deconfinement in the heavy-ion collisions. The design goals of the CMS detector were formulated in the CMS Technical Proposal [1]:

1) a very good and redundant muon system,
2) the best possible electromagnetic calorimeter consistent with 1),
3) a high quality central tracking to achieve 1) and 2).

This strategy emphasizes the primary importance of identification and precise momentum measurements of muons, electrons, and photons, resulting in an excellent mass resolution needed for discovery of the new particles ranging from the Higgs Bosons to a possible Z' boson in the multi-TeV mass range. The CMS detector was designed following the formulated above strategy. Fig. 1 shows the general view of this detector.

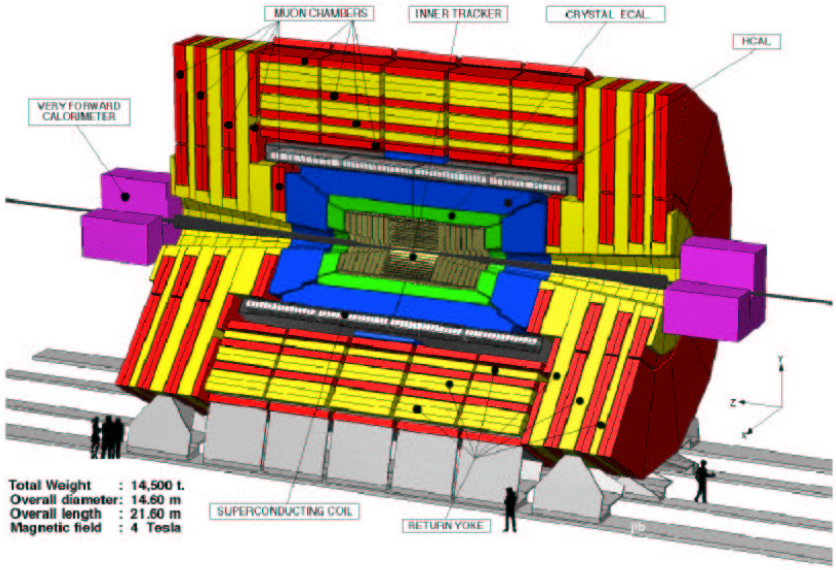

Fig. 1. 3d view of the CMS detector

2. General CMS description

2.1.Magnet and Muon System

The requirement for a compact design led to the choice of a strong magnetic field (4 T) provided by a 13 m long superconducting Solenoid of a large radius (2.95 m). Such strong magnetic field guarantees good momentum resolution for high momentum muons up to rapidities of $\eta = 2.5$, without strong demands to the muon chamber space resolution.

The Muon System [2] is embedded inside and around the magnet return yoke outside the Solenoid. It consists of two parts – Barrel and Endcaps, each containing four Muon Stations. The basic element of the Barrel are Drift Tubes (DT). There are 12 layers of DTs in each muon station. They provide 8 measurements of the $(R\Phi)$ coordinate and 4 measurements of the Z-coordinate of the muon track. The structure of the staggered DT layers allows to determine bunch-crossing for each track. In total, the Barrel Muon System contains 195,000 drift tubes.

The detector technology chosen for the Endcap Muon System (EMU) is the Cathode Strip Chambers (CSC). The trapezoidal shape of strips allows to measure the Φ-coordinate in a natural way, while the R-coordinate is provided by the signals from the wires. Each Muon Station contains six layers of CSCs, which provide the required space resolution and determine the bunch-crossing for each track. Overall, the Endcap Muon System consists of 540 six-plane trapezoidal chambers.

In addition to the Drift Tubes, Barrel will contain 6 layers of RPCs (resistive plate chambers) that should provide independent measurements of the muon arrival time. Four layers of RPC will be also in some part of the Endcap, just for redundancy as the CSCs provide the timing by themselves.

The Muon System has three functions: muon identification, muon momentum measurement, and muon trigger with well defined P_T thresholds from a few GeV to 100 GeV up to $\eta = 2.1$. The momentum resolution in the stand-alone mode $\delta P_T/P_T$ is 8 to 110 GeV and 20 to 40% at 1 TeV. The global momentum resolution after matching with the Central Tracker is 1 to 1.5% at 10 GeV and 6 to 17% at 1 TeV. The sign of the muon charge will be determined up to the kinematics limit of 7 TeV.

2.2. Central Tracking

The CMS tracking system is designed to reconstruct high P_T muons, isolated electrons and hadrons with high momentum resolution and an efficiency better than 98% in the range of $|\eta| < 2.5$. It is also designed to allow the identification of tracks coming from detached vertices from decays of b-quarks which provide very useful signatures for a broad spectrum of new physics. The CMS collaboration decided to build the Central Tracker entirely of Si-strip and Si-pixel detectors. In the barrel part, there will be 3 layers of pixel detectors surrounded with 10 layers of strip detectors. Similarly, in the endcap there will be 3 layers of pixels followed by 7 rings of strip detectors. Four layers of the strip detectors are double-sided with stereo strips to measure the coordinate in the non-bending plane. The system should provide up to 13 measured points of the track in the bending plane.

In total, there will be 9.6×10^6 readout channels from the strip detectors. In addition, the system will read out about 10^8 pixels. The whole volume occupied by the Central Tracker

is 24.4 m^3 (D = 2.4 m, L = 5.4 m), and it will be operated at low temperature (–10°C) to reduce the radiation damages. The system will provide pattern recognition at the highest LHC luminosity with the cell occupancy below 1%. The impact parameter resolution at high P_T will be of order 20 μm in the transverse plane and 100 μm in the Z-direction.

2.3. Electromagnetic calorimeter

CMS has chosen a scintillating crystal calorimeter based on lead tungsten crystals ($PbWO_4$). These crystals offer excellent energy resolution due to high density (8.28 g/cm^3), a small Moliere radius (2.0 cm), a short radiation length (0.89 cm), a quite fast (~10 ns) output signal, capability to operate in high radiation environment. Electromagnetic Calorimeter (ECAL) consists of the Barrel part ($|\eta| < 1.48$) and the Endcaps ($1.48 < |\eta| < 3.0$) with 61200 and 21528 crystals, respectively. The length of the crystals is 230 mm corresponding to $25.8X_0$. The crystal volume amounts to 8.14 m^3 (67.4 tons) in the Barrel and to 3.04 m^3 (25.2 tons) in the Endcaps. In front of the endcap crystals, there will be a Preshower Detector with the function to provide better π°-γ separation. It contains two lead converters of a thickness of $1X_0$+$1X_0$ followed by two detector planes of silicon strips. The number of read out channels will be 144384. The Si-detector will be operated at –5°C to reduce the radiation damage effects. The light from the crystals will be detected by the Silicon Avalanche Photodiodes (APDs) in the Barrel and by the more radiation hard Vacuum Phototriodes (VPTs) in the Endcaps. The light output from each crystal will be monitored by a light injection system. In addition, there will be the high precision "In situ" absolute calibration with isolated electrons from decays of W and Z bosons and b quarks.

The expected energy resolution of ECAL is:
$\sigma/E = 2.7\%/\sqrt{E} \oplus 0.21/E \oplus 0.55$, Barrel;
$\sigma/E = 5.7\%/\sqrt{E} \oplus 0.92/E \oplus 0.55\%$, Endcap, where E is given in GeV.

2.4. Hadron calorimeter

The Hadron calorimeter (HCAL) plays an essential role in the identification of quarks, gluons, and neutrons by measuring the energy and direction of jets and of missing transverse energy flow in events. Missing energy forms a crucial signature of new particles, like the supersymmetric partners of quarks and gluons. The HCAL consists of the Barrel (HB) and the Endcap (HE) parts which sit inside the Solenoid and cover the pseudorapidity range $|\eta| < 1.4$ and $1.4 < |\eta| < 3.0$, respectively. In addition, there is a Very Forward Calorimeter (VF) covering the region $3.0 < |\eta| < 5.0$. The HB and HE calorimeters consist of a set of copper absorber plates interleaved with 4 mm thick scintillator sheets. The wave-shifting fibers are imbedded into scintillator plates. These fibers deliver the light to photodetectors. Two types of photodetectors are considered: the semiconductor Avalanche Photodiodes (APDs) and the proximity focused hybrid photodiodes (PFHPDs). The VF calorimeter is located at ±11 m from the interaction point. This calorimeter should operate in extremely hard radiation conditions. A super radiation-hard technology is chosen for the VF calorimeter. It will consist of Cu plates with quartz fibers imbedded into the plates and running parallel to the beam direction. The quartz fibers will detect the Cherenkov light emitted by the fast charged particles created in the shower and transmit it to the PMTs. There will be around 2000 read out channels in each of

the two VF calorimeters. The expected energy resolution of the Hadron Calorimeter is around $\sigma/E \cong 100\%/\sqrt{E} \oplus 5\%$ over the whole η-range covered by the HCAL.

3. Development of photodetectors for CMS Endcap Electromagnetic Calorimeter

ECAL will operate in severe radiation environment. These conditions impose strong requirements for the choice of photodetectors. In addition, these detectors should provide some gain ($\sim$10) of the signal amplitude to compensate the relatively low light yield of $PbWO_4$, and they should be able to operate in the 4T magnetic field. After extensive studies, the preference was given to the Silicon Avalanche Photodetectors (APD) in the Barrel and to the more radiation hard Vacuum Phototriods (VPT) in the Endcap.

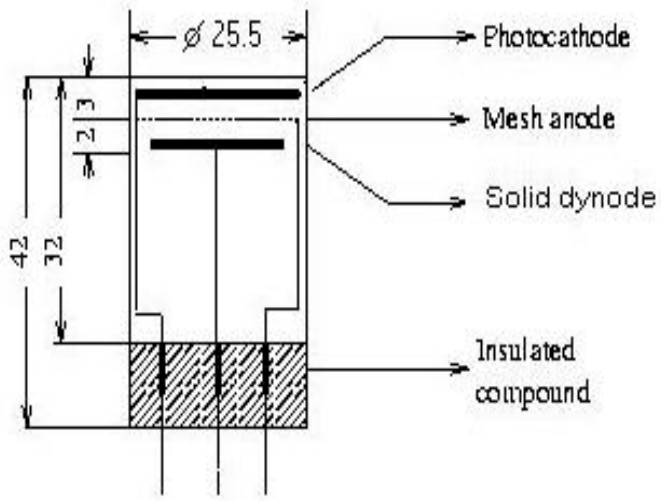

Fig. 2. Electrode layout of VPT FEU-188. Photocathode is grounded, $U_a = 100$ V, $U_d = 800$ V

PNPI in collaboration with the Research Institute Electron (RIE, St. Petersburg) performed R&D studies of various kinds of VPT produced at RIE [3]. These studies resulted in construction of a VPT (FEU-188) with parameters optimized for application in the CMS Endcap ECAL. The electrode layout of the VPT FEU-188 is shown in Fig. 2.

The quantum efficiency of the photocathode is around 20%. A large fraction of the photoelectrons liberated from the photocathode pass through the anode mesh and impact on the dynode, where they produce secondary electrons. The secondary electrons are attracted to the anode mesh where a substantial fraction is captured. The resulted gain of the VPT proved to be $G = 10$–12. The gain is little sensitive to variations of the anode voltage ($dG/G = 0.1\%$ per one Volt variation) which is one of the advantages of the VPTs. The other advantages are low sensitivity to ionizing particles, small input capacity, fast signal (1 ns).

It was very important to minimize dependence of the VPT gain on magnetic field. In FEU-188 this was achieved owing to the reduced inter-electrode space and to the very small anode mesh cell. Figs. 3, 4 show the VPT gain measured in various magnetic fields up to $B = 4$ T and

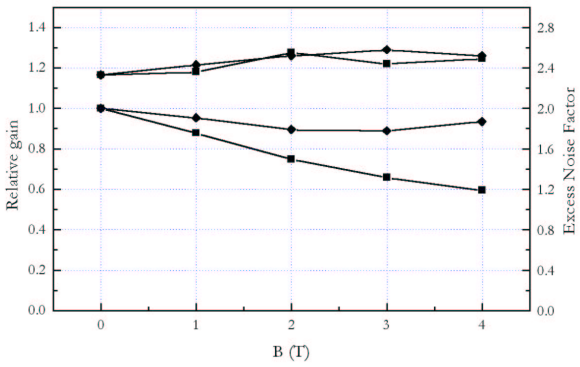

Fig. 3. Relative gain (low part of Fig.) and excess noise factor of VPT FEU-188 N2104 (top part) as a function of magnetic field for tilt angle 0° (squares) and 15° (rhombus)

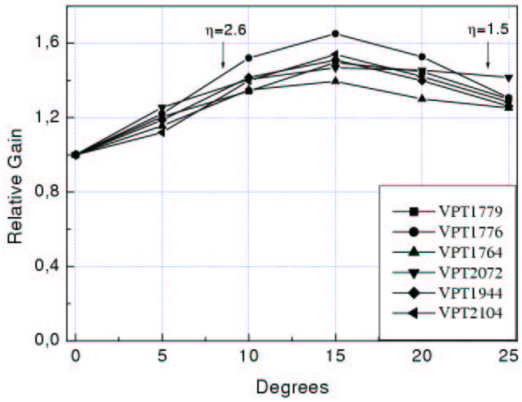

Fig. 4. Relative gain of VPT at $B = 4$ T as a function of tilt angle for a number of VPT. Arrows show the interval of η in Endcap ECAL

at various angles between the magnetic field and the VPT axis. Also shown is the excess noise factor F broadening the amplitude distribution of the signals from N photoelectrons according to $dA/A = \sqrt{F/N}$. These results are considered as quite satisfactory.

A sample of 500 VPTs was produced at RIE, and it was demonstrated that all the VPI parameters are well reproducible. The radiation hardness of the VPTs was demonstrated in the gamma irradiation tests. It was shown that the signal amplitude degrades only by 7% after the irradiation dose of 20 kGy (maximum dose for 10 LHC years), this degradation being determined mostly by some deterioration of the light transmittance of the faceplate.

Further tests of the VPT FEU-188 were performed at CERN with a full- size ECAL prototype (5×5 $PbWO_4$ crystals). The energy resolution obtained in the beam tests was: $\sigma/E = 6.5\%\sqrt{E} \oplus 122MeV/E \oplus 0.29\%$ which is close to the designed parameters.

All these studies demonstrated that the constructed VPTs satisfy the requirements of the Endcap ECAL. Based on these results, the CMS collaboration has taken decision to equip the Endcap ECAL with FEU-188 and signed a contract with RIE for production of 16,000 VPTs.

4. Development of the Endcap Muon System

The main PNPI responsibility in the CMS project is participation in design, construction and operation of the Endcap Muon System (EMU). The overall view of one quadrant of the Muon System is shown in Fig. 5.

540 cathode strip chambers are placed between the iron disks which return the magnetic flux of the central solenoid and also shield the chambers. The chambers are arranged to form four disks, called stations ME1, ME2, ME3, ME4. The station ME1 has three rings of chambers (ME1/1, ME1/2, ME1/3), while the other three stations are composed from two rings of chambers (MEn/1 and MEn/2). Each cathode strip chamber is a six-plane chamber of trapezoidal shape with a length from 1.7 to 3.4 m and with a width from 0.6 to 1.5 m. Cathode planes are formed by honeycomb panels with copper clad FR4 skins. Gas gaps defined by the panels are 9.5 mm thick. Strips run radially in the endcap geometry and provide the Φ-

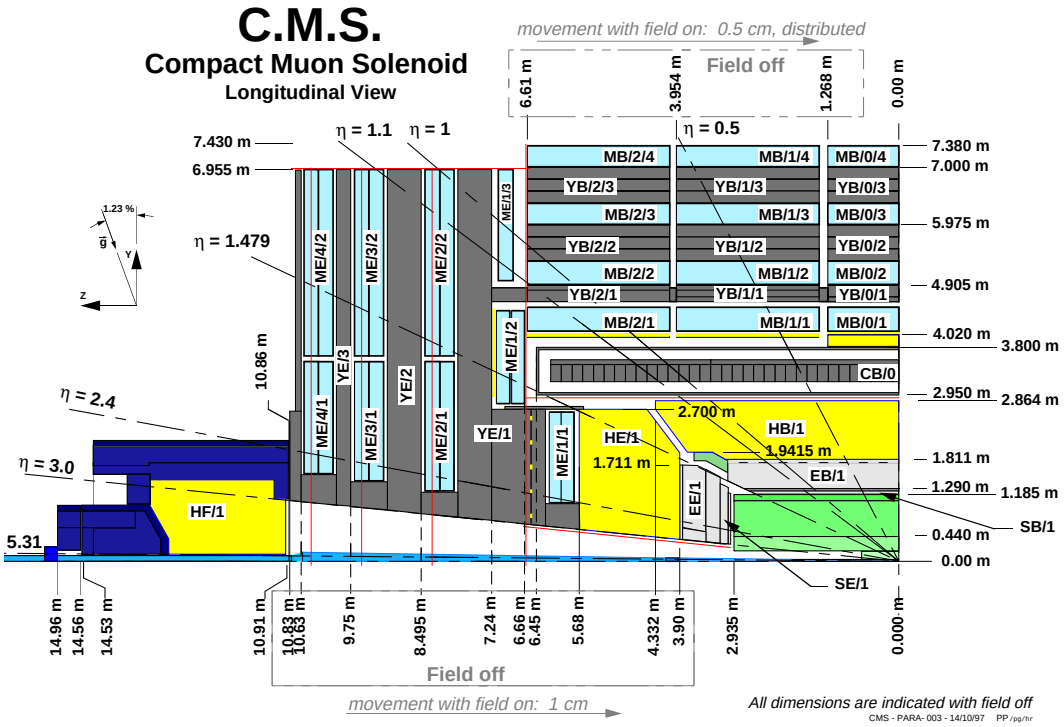

Fig. 5. View of a quadrant of the CMS Muon System

coordinate of muon hits with an accuracy of 150 μm. Wires are stretched across strips without intermediate supports and, for readout purposes, are grouped in bunches from 5 to 16. They provide the radial coordinate of muon hits with a few cm precision defined by the wire group width. Close wire spacing of 3.16 mm allows for fast chamber response within 25 ns.

In total, the EMU chambers contain about 2.5 million wires grouped into 210,816 anode channels. Also, there are 273,024 cathode channels.

PNPI participation in development of the EMU system covers:

– R& D studies of the EMU chambers (investigation of the gas mixtures, aging, chamber performance) [4–6];

– design of all EMU chambers;

– construction of the muon chambers for stations ME2/1, ME3/1, and ME4/1;

– design and production of the anode front-end electronics;

– development of the multi-channel High Voltage system;

– development of the First-Level muon trigger;

– installation and commissioning of the EMU chambers at CERN;

– maintenance of the EMU chambers throughout the lifetime of the detector.

During the construction period, the total of 114 chambers (38 of ME2/1, 38 of ME3/1, and 38 of ME4/1 type) should be fully assembled and tested with on-chamber electronics at PNPI and then delivered to CERN. To provide this mass production of the muon chambers, a clean area of 500 m^2 was prepared and equipped with special equipment developed jointly by PNPI and US-CMS specialists which includes a wire-winding machine, a wire pitch and tension measuring machine, gluing and cleaning facilities, various special tooling, various test facilities.

Mass production of the muon chambers at PNPI started in October 2001 and by the mid of July 2002 first 36 ME2/1 chambers were successfully assembled . Figs. 6–9 illustrate some of the assembling facilities at the PNPI EMU Factory.

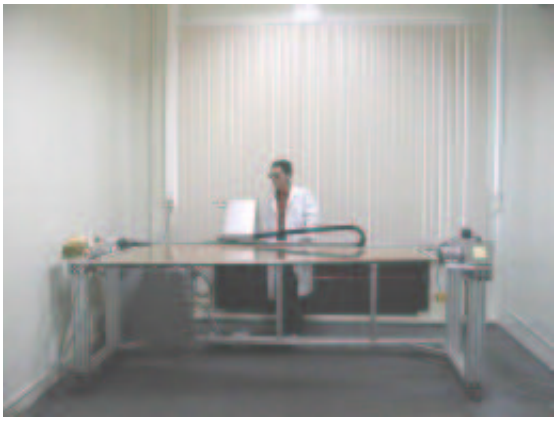

Fig. 6. Wire-winding machine

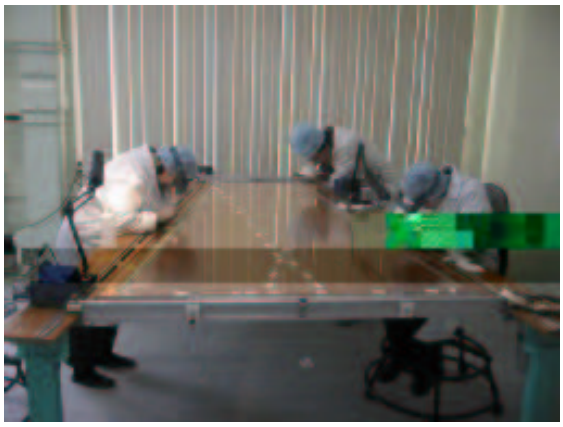

Fig. 7. Wire soldering

Fig. 8. Wire pitch and tension control

Fig. 9. Assembling of the six-layer EMU chambers

5. High Voltage System for the Endcap Muon Chambers

PNPI engineers performed a design of the multi-channel High Voltage System for the EMU chambers. Each EMU chamber contains six planes which are divided into 3 to 6 segments requiring independent current monitoring and voltage regulation. In total, this makes more than 8000 independent HV-channels. The requirements formulated for the HV-system are listed in Table 1. In addition, the system should be able to operate at rather high radiation doses about 2 kRad for ionizing particles and 10^{12} neutrons/cm^2. Also, the cost of the HV system should be as low as possible. To satisfy all these requirements, a new approach has been developed at PNPI. The block diagram of the designed HV-system is shown in Fig. 10. One mainframe with six remote distribution boxes completely serves the current and voltage monitoring and voltage regulation for up to 1944 channels. Six mainframes with thirty-two distribution boxes should be used to serve the 8000 channels of the EMU Muon System. The mainframe contains the HV power supplier and the LV power suppler to feed all 1944 channels. The industrial computer allows data to be read from all I, U sensors and control constants to be downloaded to the linear regulators.

Table 1

High voltage system parameters

Parameter	**Required**	**Achieved**
Maximum input voltage	4000 V	4000 V
Voltage regulation, chamber	0 to 4000 V	0 to 4000 V
Voltage regulation, each segment	from U_{max}–500 V to U_{max}	from U_{max}–2000 V to U_{max}
Voltage regulation step	$\leq$ 50 V	1 V
Ripple and noise	10 mV p-p, 100 Hz–20 MHz	10 mV p-p, 100 Hz–20 MHz
Voltage measurement resolution	10 V	1 V
Maximum output current, one output	100 μA	100 μA
Total output current	40 μA$\times N$ channels	40 μA$\times N$ channels
Current measurement resolution	100 nA	2 nA for $I \leq 1\mu$A, 100 nA for $I \geq 1\mu$A
Trip level	1 μA to 100 μA	1 μA to 100 μA
Trip level setting step	1 μA	1 μA
Connection to SCADA	Yes	Yes
Individual channel turn-off speed	$\leq$ 10 ms	$<$ 10 ms

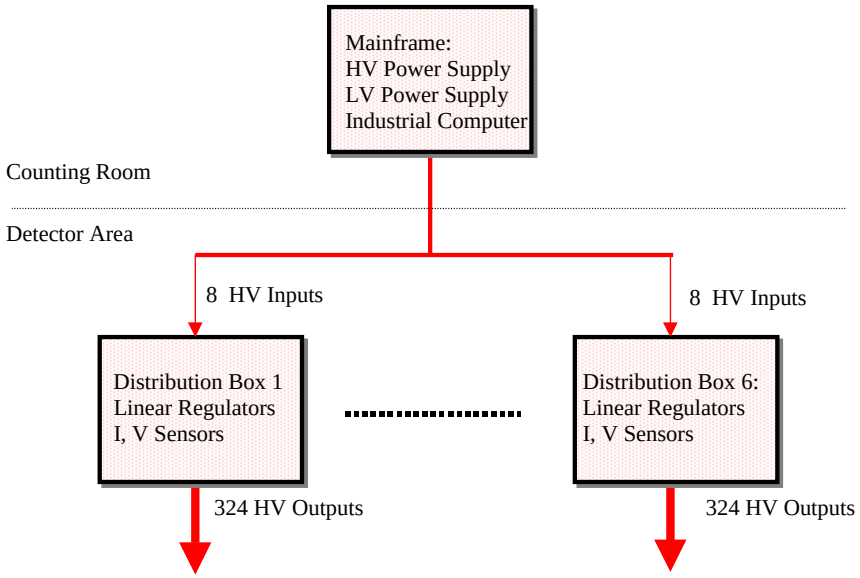

Fig. 10. Block diagram of High Voltage System

Forty eight long mainframe to distribution boxes to be fan-out to 1944 short HV cables. The short HV cables are connected to the chamber segments. A 32-channel prototype has been constructed and tested showing very good results, except not sufficient radiation hardness. This problem was solved in the second prototype. Also, this prototype contained some modifications decreasing the cost of the HV-system. The parameters achieved with these prototypes are presented in Table 1. The decision on mass production of the HV-system distance HV cables are coming from each will be taken by CMS collaboration in 2003.

6. Anode front-end electronics for muon chambers

The EMU muon chambers have readout both from the cathode strips and from the groups of anode wires. The PNPI engineers in cooperation with Carnegie Mellon University were responsible for design and production of the anode front-end electronics. The FE electronics should provide the best possible time resolution operating with large detector capacitance (up to 200 pF) and with large signal rates up to 20 kHz/channel. It should be reliable during for 10 LHC years receiving radiation dosage about 2 kRad for ionizing particles and about 10^{12} neutrons per cm^2 . Also, it should have low power consumption. Total number of the anode channels is more than 150,000. As the result of more than five year efforts, the electronics satisfying all these requirements has been designed and fabricated. Each electronics channel consists of an input protection network, amplifier, shaper, constant-fraction discriminator, and a programmable delay line with an output pulse width shaper (Fig. 11). An essential part of the electronics is an ASIC (CMP16 chip) consisting of a 16-channel amplifier-shaper-discriminator. This chip (Fig. 12) was designed using a BiCMOS 1.5 micron technology, and it was produced in the USA industry. Its main characteristics are presented in Table 2. An important feature of CMP16 is the two-threshold constant-fraction discriminator allowing to keep the noise rate at a low level not deteriorating the time resolution. The second designed ASIC (DEL16 chip) provides a programmable time delay which allows the time alignment of the signals with the delay step of 2 ns (15 steps maximum).

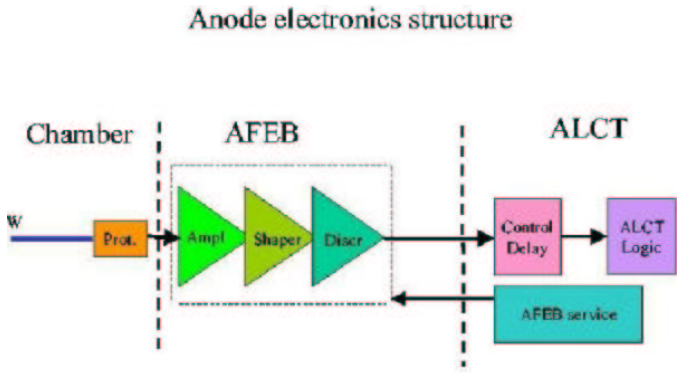

Fig. 11. Anode electronics structure. Protection board (Prot.) is a part of the chamber assembly, AFEB – Anode Front-End Board is a 16-channel board, ALCT – Anode Local Charge Track finder logic board

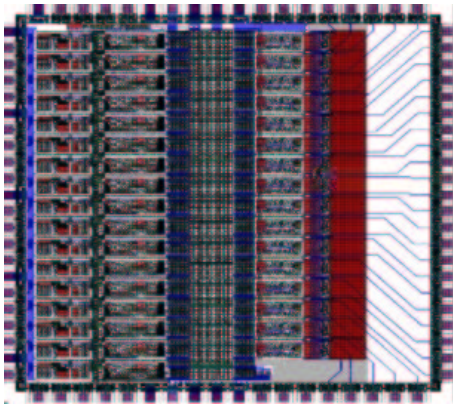

Fig. 12. CMP16 ASIC chip layout

On the basis of the CMP16 chip, a 16-channel Anode-Front-End Board AD16 was designed. This board receives the anode signals from the chamber wire groups, amplifies the signals, selects the signals over the preset threshold with precise time accuracy and transmits the logic level signals to the further stage with the LVDS levels standard. The EMU system contains almost 10,000 AD16 boards. The designed AD16 board passed through various reliability and radiation tests demonstrating quite satisfactory behaviour under conditions of the CMS experiment. After that, the mass production of the CMP16 and DEL16 chips as well as the AD16 boards has been started, and by mid of 2002 all the electronics (22,000 chips and 12,000 boards) has been produced. The detailed tests of the major part of the produced electronics showed good

Table 2

Electrical parameters of the CMP16 chip

Input impedance	40 Ω
Transfer function	7 mV/fC
Shaper peaking time	30 ns
Amplifier input noise	0.5 fC @ $C_{in} = 0$; 1.7 fC @ $C_{in} = 200$ pF
Two-threshold discriminator: High-level threshold Low-threshold	 Adjustable 0–100 fC zero-crossing discriminator
Power supply voltage	5 V
Power consumption	0.5 W/chip

results. By the end of 2002 all the anode FE electronics will be ready for installation on the EMU muon chambers.

7. Track-Finding Processor for Level-1 Trigger of the Endcap Muon System

PNPI engineers in cooperation with University of Florida are responsible for design and production of the Track-Finding Processor for EMU system [7]. The Track-Finder is implemented as 12 sector processors which identify up to three best muons in 60° azimuthal sectors. The track-finding algorithms are inherently 3-dimensional to achieve maximum background rejection. The purpose of the Track-Finding Processor is to link track segments from individual muon stations into complete tracks, to measure the transverse momentum P_T from the sagitta induced by the magnetic bending, and to report the number and quality of the tracks to the Level-1 global trigger.

The block diagram of the Track-Finding Processor is shown in Fig. 13. The input of the processor is capable of collecting track segments from multiple bunch crossings (BX). The bunch

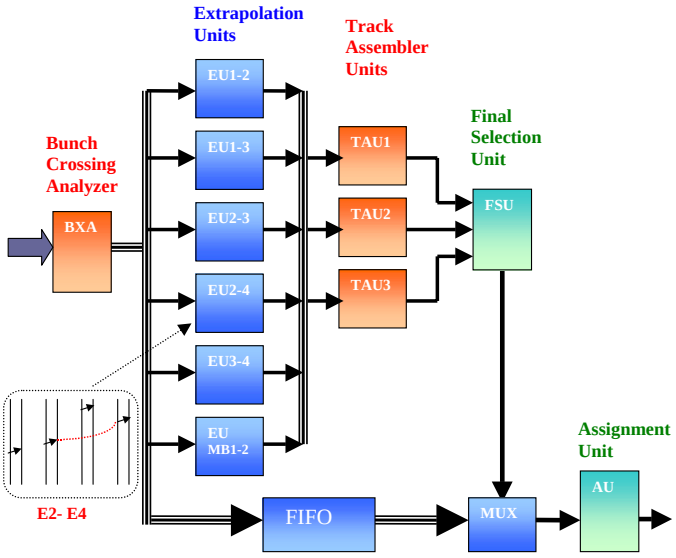

Fig. 13. Block diagram of the Track-Finding Processor

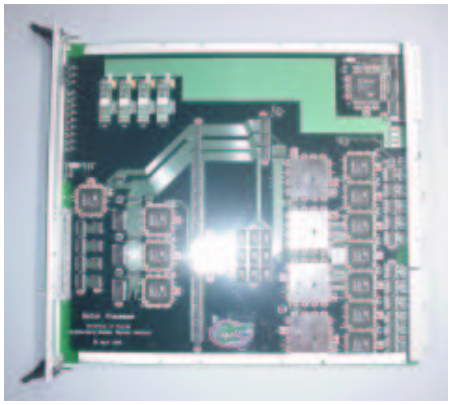

Fig. 14. First prototype of the Track-Finding Processor

crossing analyzer accumulates track segments for a couple of BX to accommodate error in BX. The extrapolation unit takes information from two track segments in different stations and tests if those two segments are compatible with the muon originating from the nominal collision vertex with a curvature consistent with the magnetic bending in that region. The track assembler units examine the output of extrapolation units and determines if any track segment pairs belong to the same muon. The final selection unit combines the information from track assembler streams, cancels redundant tracks, and selects the three best distinct tracks. The assignment unit measures the momentum of the identified muons in the final stage of the processing. The overall latency of processor is expected to be about 175 ns. The first prototype of the processor (Fig. 14) has been fabricated in 2000 and successfully tested in 2000–2001. This is a 9U VME module 400 mm depth. There are 17 Field Programmable Gate Array (FPGA) chips as core elements of the module. The pre-production prototype of the processor is under design. The new processor occupies only one big size FPGA chip. It allows to reduce the processing time from 375 ns (first design) to 175 ns. It also allows to combine three sector receivers and the processor on one board to reduce the total number of modules from 48 to 12. According to the schedule, the PCB layout of the pre-production prototype will be completed by September, 2002. The fabrication of the pre-production prototype will be finished by November 2002, and testing should be done by April 2003.

PNPI participants in the CMS project:

A.A.Vorobyov, D.M.Seliverstov, Yu.M.Ivanov, V.L.Golovtsov, V.S.Kozlov, O.E.Prokofiev, A.G.Atamachuk, V.Baldychev, Yu.S.Blinnikov, N.F.Bondar, A.S.Denisov, G.E.Gavrilov, V.V.Golubev, A.G.Golyash, G.A.Gorodnitsky, D.Gulevich, N.M.Gulina, Yu.I.Gusev, M.R.Kan, V.T.Kim, A.I.Kovalev, A.N.Koznov, A.G.Krivchitch, Z.G.Kudryashova, E.V.Kuznetsova, L.P.Lapina, V.I.Lazarev, V.D.Lebedev, T.B.Lebedeva, I.A.Levityansky, L.A.Levtchenko, P.M.Levtchenko, E.A.Lobachev, G.V.Makarenkov, F.V.Moroz, E.M.Orischin, A.A.Petrunin, B.V.Razmyslovich, V.G.Razmyslovich, A.I.Schetkovsky, L.A.Schipunov, V.N.Sedov, V.A.Sknar, S.Slizovsky, I.B.Smirnov, N.M.Stepanova, V.V.Sulimov, V.I.Tarakanov, I.I.Tkatch, L.N.Uvarov, S.A.Vavilov, G.N.Velitchko, S.S.Volkov, D.O.Yakorev, V.I.Yatsura.

References

[1] The Compact Muon Solenoid. Technical Proposal, CERN/LHCC 94-38, 15 Dec. 1994.

[2] The CMS Muon Project. Technical Design Report, CERN/LHCC 97–32, 15 Dec. 1997.

[3] N.A.Bazhanov *et al.*, Nucl. Instr. Meth. **A442**, 146 (2000).

[4] T.Ferguson, G,Gavrilov, A.Korytov, A.Krivchitch, E.Kuznetsova, E.Lobachev, G.Mitselmakher, and L.Schipunov, Preprint PNPI-2442, 2001, Gatchina.

[5] G.Velichko, CMS Note 2000/022.

[6] R.Breedon, ..., O.Prokofiev *et al.*, CMS IN 2000/004.

[7] D.Acosta, A.Maforsky, B.Scurlock, S.M.Wang, A.Atamanchuk, V.Golovtsov, and B.Razmyslovich, CMS Note 1999/060, 8 Dec. 1999.